Catalysis Letters
https://doi.org/10.1007/s10562-018-2580-4

Peptide Nanofiber Templated Zinc Oxide Nanostructures as Non-precious Metal Catalyzed *N*-Arylation of Amines, One-Pot Synthesis of ImidazoHeterocycles and Fused Quinazolines

Zahra Taherinia[1] · Arash Ghorbani-Choghamarani[1] · Maryam Hajjami[1]

Received: 23 July 2018 / Accepted: 26 September 2018

Abstract
In the present study, peptide nanofiber was used to immobilize zinc oxide. This nanoparticle was prepared through self-assembly in an aqueous solution. The structural properties of the prepared catalyst were examined by a series of techniques, such as FT-IR, EDS, SEM, TEM, XRD, ICP-OES (inductively coupled plasma optical emission spectrometry), and ultraviolet–visible (UV–Vis) spectroscopy. TEM images showed the necklace model for peptide nanofiber decorated with zinc oxide. The versatility of the method was investigated by *N*-arylation using reaction of amines with hydroxybenzotriazole as a novel phenylating reagent, one-pot synthesis of imidazoheterocycles by a three-component reaction of 2-aminopyridine, aldehyde, terminal alkyne *and* preparation of tetracyclic quinazolinone ring by one-pot reaction of isatoic anhydride, amine, and ninhydrin. High yields, low cost of catalyst, environmental friendliness, efficient recovery and recyclability of catalyst are the most important features of this catalytic system.

Electronic supplementary material The online version of this article (https://doi.org/10.1007/s10562-018-2580-4) contains supplementary material, which is available to authorized users.

✉ Arash Ghorbani-Choghamarani
arashghch58@yahoo.com; a.ghorbani@ilam.ac.ir

[1] Department of Chemistry, Faculty of Science, Ilam University, P.O. Box 69315516, Ilam, Iran

Published online: 12 October 2018

Graphical Abstract

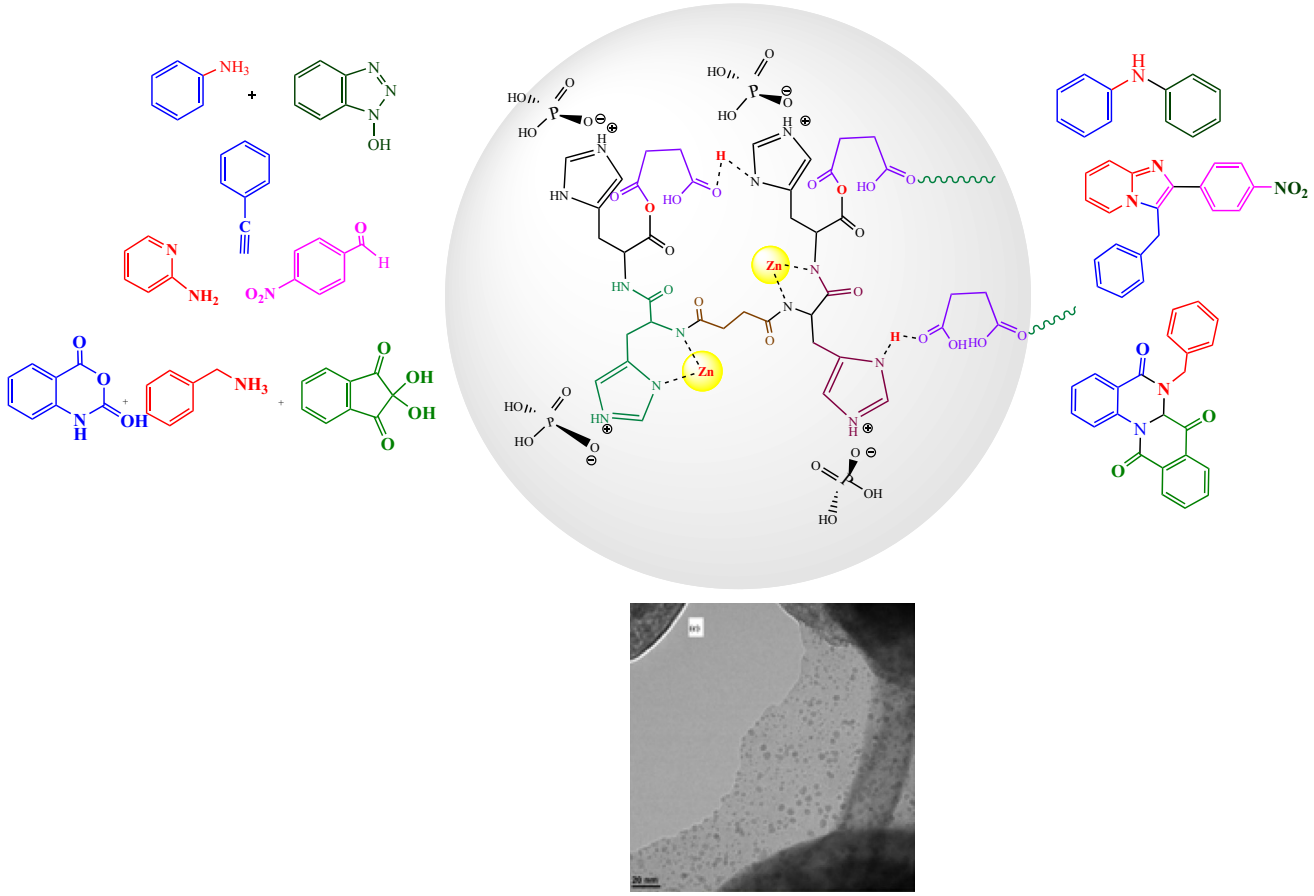

Keywords Peptide nanofiber · Hydroxybenzotriazole · ZnO nanoparticles · Tetracyclic quinazolinone · Imidazo [1,2-a] pyridine

1 Introduction

The catalytic formation of carbon–heteroatoms bond has received significant interest in recent years due to its multiple applications in the pharmaceutical, natural products, organic materials and dye industries [1, 2]. The cross-coupling of amines with aryl halides to their corresponding C–N is the most common method in the presence of stoichiometric or catalytic amounts of either copper [3] or palladium [4]. for *N*-arylation formation. Although these methods are very effective, they have drawbacks. For example, aryl halides are generally environmental pollutants, and syntheses are carried out in the presence of expensive noble metals, needing of stoichiometric amounts of catalyst and high-temperature reaction media. *Multi-component* (*MCRs*) and domino reactions are a valuable strategy in the green chemistry and involve the combination of more than two components in a single synthetic operation [4]. The major advantages of MCRs include atom efficiency, high selectivity, and reduction of the generation of chemical waste, environmental [5].

Imidazo [1,2-a] pyridine and tetracyclic quinazolinone are an emerging class of heterocycles, which is extensively investigated for useful pharmaceutical activity [6] and biological activity [7]. A variety of methods have been developed for preparation of imidazo [1,2-a] pyridines imidazole. Of these, multicomponent reactions (MCRs) involve the one-pot combination of three component coupling (3CC) of 2-aminopyridine, aldehyde, and alkyne is one of the most attractive methods for the synthesis of imidazo [1,2-a] pyridines. A number of transition metal salts such as Ag(I) [8], $InBr_3$ [9], Au(III) [10], and Cu(II) [11, 12] have been employed to accomplish this three-component coupling for the synthesis of imidazo [1,2-a] pyridines.

Quinazolinones are important class of fused heterocyclic alkaloids showing a wide range of biological [13] and pharmacological activities [14]. Consequently, methods have been reported for the synthesis of tetracyclic quinazolinone:

(i) the condensation of isatoic anhydride and amine with ninhydrin in aqueous HCl [15], (ii) utilizing palladium-catalyzed carbonylation of commercially available 2-bromobenzyl amine and 2-bromoaniline as the starting materials [16]. Although all of these methods are beneficial, a number of them have one or more of the following drawbacks: tedious workup of the reaction mixture, long reaction times, low yields of products, expensive metal and difficulty in separation and recovery of the catalyst. Hence, the choice of a suitable catalyst and environmentally benign method that avoids all of these drawbacks is of key importance to get good results. The great interest in catalysis using nanomaterials due to increased accessibility to surface atoms has prompted the synthesis and investigation of diverse highly functionalized NPs. Since NPs easily agglomerate and oxidize due to high surface energy in aqueous solution, in many cases, metal nanoparticles are immobilized on the various support, such as zeolites [17], boehmite [18], dendrimers [19], silicates [20], activated carbon [21] and nanofiber [22].

Nature-inspired peptide nanofiber networks have wide applications for biomedical such as drug delivery [23], vaccinations [24], and tissue engineering [25]. Interactions among peptide-based nanostructures can lead to the formation of various functional nanostructures such as nanotubes, spherical vesicles, nanofibrils, nanowires, and necklaces. The self-assembled peptide is formed by inter- and intramolecular forces such as hydrogen bond formation, hydrophobic and electrostatic interactions, van der Waals forces, and π–π stacking and this process is controlled by the balance of attractive/repulsive forces within and between molecules. Recent reports show that a nanostructured peptide has been used as a template to stabilize metal nanoparticles and to prevent aggregation of the nanoparticles [26]. For example, Maity et al. [27] reported peptide nanofiber-supported palladium nanoparticles as an efficient catalyst for the removal of N-terminus protecting groups, and Wang et al. [28] reported the synthesis of a new hairpin peptide decorated with copper(II), which were utilized as templates for the synthesis of long, ultrathin CuS nanowires. Moreover, Acar et al. [29] demonstrated peptide nanofiber templated synthesis of TiO_2 nanostructures, Khalily et al. [30] reported bioinspired supramolecular peptide nanofiber templated Pd^0 hybrid nanocatalyst and Kim et al. [31] reported the synthesis of a sphere-to-bridge-shaped peptide nanostructure was constructed from a tyrosine-rich peptide (HYYACAYY-OH) via mediating Pd^{2+} ions as an efficient catalyst for the Suzuki coupling reaction. In this context, efforts have been directed toward other synthetic methods, which include noteworthy features such as low price and efficient catalytic activity, being reusable more than once and free-from aryl halide. In our previous report [22], we developed the synthesis of biphenyls using the reaction of aryl halides with hydroxybenzotriazole as a novel *phenylating agent*. Herein we would like to describe the *N*-arylation reaction using hydroxybenzotriazole, one-pot synthesis of imidazoheterocycles by a three-component reaction of 2-aminopyridine, aldehyde and terminal alkyne *and* tetracyclic quinazolinone ring synthesis from isatoic anhydride, amine, and ninhydrin in the presence of peptide nanofiber decorated with ZnO. In this regard, we describe approaches based on the self-assembly of peptide-histidine (Fig. 4) has been shown to be an effective template for catalysts due to their high surface area-to-volume ratio, giving the reactants easy access to a large number of active sites.

2 Experimental Section

2.1 Materials

All reactants were purchased from Merck and Aldrich Chemical Company and used without further purification.

2.2 Preparation of Histidine Ethyl Ester Hydrochloride (1)

In our experiment (6.0 mL, 82.1 mmol) thionyl chloride was added dropwise to a stirred mixture of histidine (54.7 mmol) in Ethanol (100 mL) at 0 °C. The mixture was stirred for 24 h at room temperature. The precipitate was removed by filtration. The crude product was purified by recrystallization using EtOAc/EtOH (80:20) to give a white solid [30]. FT-IR (KBr) ν_{max}/cm^{-1}: 1392, 1479, 1586, 1622, 1738, 2570, 2793, 2883, 3019, and 3100.

2.3 Synthesis of Compound (2)

In a typical procedure, 0.5 g (5 mmol) succinic anhydride was dissolved in 3 mL of DMF in an ice-water bath and stirred for 5 min. Followed by adding (5 mmol) of histidine ethyl ester hydrochloride, subsequently (5 mmol) *N*-methyl morpholine was added to this mixture. The resultant was stirred for overnight. Finally, 50 mL ethyl acetate was added to the reaction mixture and the resulting precipitate was removed by filtration and purified by recrystallization using EtOAc/EtOH (80:20) to yield compound **2** as a white solid [30]. FT-IR (KBr) ν_{max}/cm^{-1}: 1073, 1125, 1179, 1225, 1339, 1419, 1494, 1644, 1736, and 3415.

2.4 Synthesis of Compound (3)

The compound **2** (3.5 mmol) in 3 mL of DMF was stirred in an ice-water bath, then (7 mmol) of histidine ethyl esterhydrochloride was added to this mixture. In the next step ethyl acetate (10 mL) was added followed by mixing with 0.68 g (3.85 mmol) DCC and 0.520 g (3.85 mmol) of HOBt. Afterward, the reaction mixture was stirred overnight and

washed repeatedly with ethyl acetate to remove DCU. The crude product was purified by recrystallization using EtOAc/EtOH (80:20) to give a white solid [30]. FT-IR (KBr) ν_{max}/cm^{-1}: 693, 936, 999, 1289, 1399, 1454, 1622, 1655, 1839, 1926, 2045, 2265, 2548, 2925 and 3086.

2.5 Synthesis of Compound (4)

To a round bottom flask, containing (2.7 mmol) of compound **3**, EtOH (6 mL), 2 M NaOH (2 mL) was added dropwise. The reaction mixture was stirred overnight. After completion of the reaction, the pH was adjusted to 1 by dropwise addition of 1 M HCl followed by addition of the ethyl acetate (50 mL). After filtration and removal of the solvent, the white solid of the desired compound produce [32]. FT-IR(KBr) ν_{max}/cm^{-1}: 1071, 1351, 1425, 1575, 1624, 1729, 2886, 3008, 3083, 3265, 3570, and 3745.

2.6 Synthesis of Compound (5)

A mixture of compound **4** (2.42 mmol) in 3 mL DMF was cooled in an ice-water bath, then (9.7 mmol) of histidine ethyl ester hydrochloride was added followed by adding 0.68 g (3.85 mmol) DCC and 0.520 g (3.85 mmol) of HOBt. Afterwards, the reaction mixture was stirred for overnight, and then *washed* repeatedly with ethyl acetate to remove any residual DCU byproduct. The solvent was removed and evaporated to provide compound **4**. The crude product was purified by recrystallization using EtOAc/EtOH (80:20) [30]. FT-IR (KBr) ν_{max}/cm^{-1}: 1075, 1132, 1184, 1339, 1405, 1462, 1491, 1631, 1737, 1842, 1929, 2616, 2704, 2888, 3099 and 3414.

2.7 Synthesis of Compound (6)

In a round bottom flask, 2 M NaOH was added drop-wise to (1.8 mmol) of compound **5** in 10 mL EtOH. The reaction mixture was stirred overnight. After completion of the reaction, the pH was adjusted to 1 by dropwise addition of 1 M HCl, followed by addition of the ethyl acetate (50 mL) filtered to provide compound **6** [32]. ^{1}H NMR (400 MHz, D_2O) δ2.84 (s, 2H), 3.25–2.96 (m, 4H, $C^{\beta}H$), 4.07–3.90 (m, 2H, $C^{\alpha}H$), 6.95 (d, $J = 9.2$ Hz, 2H, ArH), 7.67 (s, 1H, ArH), 7.89 (s, 1H, ArH), ^{13}CNMR (100 MHz, D_2O) (δ, ppm): 28.3, 29.4, 54.8, 56.4, 116.9, 117.8, 132.1, 136.4, 160.4, 163.6, 174.4, 180.1. FT-IR (KBr) ν_{max}/cm^{-1}: 1084, 1125, 1390, 1624, 1729, 2792, 2883, 3101, 3441. Anal. Calcd for $C_{28}H_{34}N_{12}O_8$: C, 49.40; H, 6.19; N, 26.21; O, 18.20.

2.8 Preparation of Peptide Nanofiber (7)

26.65 mg (0.04 mmol) of the synthesized peptide was dissolved in an aqueous solution containing 0.2 mL double distilled water and 0.8 mL phosphate buffer solution (pH 5) followed by adding 32 mg (0.31 mmol) of succinic anhydride to the peptide solution and sonicated for a few minutes. This mixture was stirred overnight at 80 °C. FT-IR (KBr) ν_{max}/cm^{-1}: 1066, 1178, 1405, 1558, 1646, 1722, 2859, 2930, 3438.

2.9 Synthesis of ZnO Nanoparticle Supported on the Peptide Nanofiber (ZnO NP-PNF)(8)

Peptide 30.14 mg (0.04 mmol) was dissolved in 0.2 mL of double distilled water. then 0.8 mL phosphate buffer solution (pH 5) was added. The solution was sonicated for a few minutes. This mixture was stirred overnight at 80 °C. In the next step $Zn(NO_3)_2{\cdot}6H_2O$ (5.94 mg, 0.02 mmol) was added to the reaction mixture and stirred for 12 h at 80 °C, to obtain ZnO NP-PNF quantitatively.

2.10 General Procedure for the Synthesis of Secondary Amines

The reaction was conducted at 130 °C in DMSO (3 mL) with the substituted amine (2 mmol), hydroxybenzotriazole (1 mmol), KOH (5 mmol) and 0. 75 mg of catalyst. The progress of the reaction was monitored by TLC. After reaction completion, the mixture was cooled to room temperature and was extracted with ethyl acetate (2 × 20 mL). The organic extract was washed twice with water and dried with anhydrous Na_2SO_4, then filtered and the solvent was evaporated to achieve corresponding aryl amine. In order to obtain high pure arylamine, the crude product purified by preparative TLC.

2.11 General Procedure for the Synthesis of Imidazoheterocycles

A catalytic amount of ZnO nanoparticle decorated on peptide nanofibers (0.75 mg) was added to a mixture of benzaldehyde (1 mmol), 2-aminoazine (1 mmol), and phenylacetylene (1 mmol). The reaction mixture was then stirred at 100 °C. Reaction progress was monitored by TLC. Upon the reaction completion, the product was extracted with ethyl acetate (2 × 10 mL). The resultant organic layer was washed with distilled water, dried over anhydrous sodium sulfate, and concentrated to give the crude solid crystalline product.

2.12 General Procedure for the Synthesis of Quinazoline Tetracyclic Derivatives

A mixture of isatoic anhydride (1 mmol), amine (1 mmol) and 0.625 mg of catalyst in PEG, was stirred at 100 °C. After the reaction was completed, ninhydrin (1 mmol) was added into the resulting mixture. Then the mixture was heated at 100 °C and the reaction was monitored by TLC for an appropriate time. After completion, the mixture was cooled to room temperature and 20 mL of ethyl acetate was added to the organic phase and *washed* with water, dried over anhydrous Na_2SO_4, and filtered. The residue was purified by column chromatography (silica gel, hexane/ethyl acetate) to afford the corresponding product.

Compound **1** (Table 2): δ ^{1}HNMR ($CDCl_3$, 400 MHz): δ = 7.96 (d, J = 7.3, 6H), 7.56–7.47 (m, 4H), 6.7 (br, 1H, NH).

Compound **5** (Table 2): δ ^{1}HNMR ($CDCl_3$, 400 MHz): δ = 7.85 (t, J = 6.8 Hz, 2H), 7.75–7.73 (m, 1H), 7.58–7.49 (m, 5H), 6.95–6.88 (m, 1H) 6.4 (s, 1H), 4.2 (s, 3H).

Compound **3** (Table 4): ^{1}H NMR (400 MHz, $CDCl_3$) δ 9.9 (s, 1H), 8.4 (d, J = 8.4, 4H), 8.12–8.10 (m, 3H), 7.8–7.72 (m, 3H), 7.35 (d, J = *8*, 1H), 7.03 (d, J = *8.8*, 1H), 3.69 (s, 2H).

Compound **4** (Table 4): ^{1}H NMR (400 MHz, DMSO) δ 9.90 (s, 1H), 7.9 (s, 1H), 7.43–7.37 (m, 2H), 7.32–7.03 (m, 3H), 6.71–6.56 (m, 3H), 6.48–6.42 (m, 4H), 3.56 (s, 2H).

Compound **5** (Table 4): ^{1}H NMR (400 MHz, DMSO) δ 8.50–8.48 (m, 2H), 7.99–7.86 (m, 4H), 7.35–7.21 (m, 3H), 6.48–6.44 (m, 3H), 3.40 (s, 2H).

Compound **1** (Table 6): ^{1}H NMR (400 MHz, DMSO) δ 8.14 (t, J = 7.6, 2H), 8.07 (s, 1H), 7.90–7.87 (m, 3H), 7.55 (d, J = 8.4, 2H), 7.55 (d, J = 8.4, 2H), 7.41 (t, J = 4.2, 2H), 4.44 (s, 2H), ^{13}C NMR (100 MHz, $CDCl_3$): δ = 180.8, 178.0, 145.0, 137.4, 137.7, 134.6, 133.6, 133.1, 127.1, 126.6, 126.5, 119.2, 117.6, 114.2, 41.1.

Compound **4** (Table 6): ^{1}H NMR (400 MHz, DMSO) δ 7.93 (d, J = 8, 3H), 7.68–7.64 (m, 3H), 7.23–7.19 (m, 4H), 2.55 (q, J = 7.4 3H), 1.5 (t, J = 7.3 3H). ^{13}C NMR (100 MHz, $CDCl_3$): δ = 188.9, 168.08, 147.0, 144.4, 142.7, 134.3, 131.8, 128.7, 128.6, 126.5, 123.7, 106.7, 28.6, 15.4. FT-IR (KBr) ν_{max}/cm^{-1}: 3062, 3023, 2926, 2849, 1714, 1652, 1477, 1435, 1408, 1161, 1091, 1019, 726, 680, 527, 462.

Compound **5** (Table 6): ^{1}H NMR (400 MHz, $CDCl_3$) δ 8.17 (d, J = 7.6, 3H), 7.66–7.62 (m, 2H), 7.29 (q, J = 6.8, 3H), 7.17 (d, J = 8, 2H), 2.77 (m, 1H), 1.32 (d, J = 8, 6H). FT-IR (KBr) ν_{max}/cm^{-1}:3024, 2924, 1708, 1630, 1503, 1511, 1408, 1312, 1249, 1033, 951, 901, 819, 737, 662, 540.

Compound **6** (Table 3): δ ^{1}H NMR (400 MHz, $CDCl_3$) δ 8.3 (t, J = 7.2, 1H), 8.2 (d, J = 7.6, 1H), 8.10–8.0 (m, 1H), 7.99–7.98 (m, 1H), 7.82–7.81 (m, 2H), 7.47 (d, J = 8.8, 2H), 2.77 (t, J = 7.8 Hz, 2H), 1.34–1.31 (m, 4H), 0.914 (t, J = 7.6, 2H). ^{13}C NMR (100 MHz, $CDCl_3$): δ = 202.6, 162.4, 152.2, 138.6, 134.9, 128.3, 123.3, 115.0, 40.9, 30.0, 20.2, 13.8.

Compound **8** (Table 6): ^{1}H NMR (400 MHz, DMSO) δ 7.8 (d, J = 8, 2H), 7.62–7.55 (m, 2H), 7.26–7.02 (m, 4H), 2.51–2.41 (m, 1H), 1.75–1.59 (m, 10H), FT-IR (KBr) ν_{max}/cm^{-1}:2927, 2858, 1726, 1655, 1475, 1429, 1374, 1302, 1255, 1185, 1075, 1019, 973, 899, 725, 680.

Compound **9** (Table 6): ^{1}H NMR (400 MHz, DMSO) δ 8.4 (s, 1H), 8.17 (d, J = 8, 1H), 8.17 (d, J = 8, 1H), 7.92 (d, J = 8, 1H), 7.84 (q, J = 4.9, 2H), 7.69–7.63 (m, 1H), 7.55 (t, J = 7.2, 1H), 7.21 (q, J = 8.5, 1H), 3.36–3.32 (m, 1H), 1.48–1.37 (m, 14H). ^{13}C NMR (100 MHz, $CDCl_3$): δ = 186.8, 159.8, 147.8, 146.6, 139.9, 135.2, 134.6, 127.5, 127.4, 126.7, 123.4, 122.8, 121.9, 115.2, 40.6, 39.3, 26.4, 26.3, 25. FT-IR (KBr) ν_{max}/cm^{-1}:3056, 3020, 2923, 2846, 1711, 1656, 1609, 1403, 1153, 1100, 1022, 942, 821, 743, 676, 537, 463.

3 Results and Discussion

A schematic illustration of the preparation strategy of the peptide nanofiber templated ZnO nanostructures (ZnNP-PNF) was shown in Scheme 1. Peptide ***6*** employed in this report was synthesized by conventional solution phase methodology. The C-terminus of amino acid was protected as ethyl ester. Couplings were mediated by dicyclohexylcarbodiimide-1-hydroxybenzotriazole (DCC-HOBt). The final compounds were purified and fully characterized by ^{1}H NMR and ^{13}CNMR spectral studies. In this work, the effect of phosphate buffer solutions on the structure of peptide nanofiber was investigated. After the peptides nanofiber was designed and synthesized $Zn(NO_3)_2{\cdot}3H_2O$ was immobilized on the surface of this nanostructural compound (Scheme 1). The structure of the ZnO nanoparticles product was elucidated on the basis of FT-IR, EDS, SEM, XRD, ICP-OES, TEM and fluorescence spectroscopy. The FT-IR spectra provide valuable information regarding the nature of the functional group attached to the metal atom. In order to study the bending mode of the peptide nanofiber decorated with ZnO, the IR spectrum of the peptide nanofiber was compared with the peptide nanofiber decorated with ZnO. Peptide nanofiber mainly exhibited four characteristic peaks at 1722, 1646, 1177, and 1067 cm^{-1}, corresponding to (C=O), (N–H), and (C–OH), respectively. However, the corresponding peaks of peptide nanofiber/ZnO were changed to 1719, 1639, 1179, and 1057 cm^{-1}. The position and intensity of characteristic

peaks were known to reflect the coordination behavior of peptide nanofiber and ZnO. We also found that there are two new peaks at 450.51–665 cm^{-1}, which were assigned to the characteristic peaks of zinc oxide nanoparticles [33] (Fig. 1). The structure and phase purity of peptide nanofiber and peptide nanofiber templated zinc oxide nanostructures were studied by X-ray diffraction analysis (XRD). Figure 2 shows the XRD pattern of nanoparticles. From the analysis of the XRD pattern of nanoparticles clearly seen that the prepared ZnO nanoparticles showed a single-phase nature with

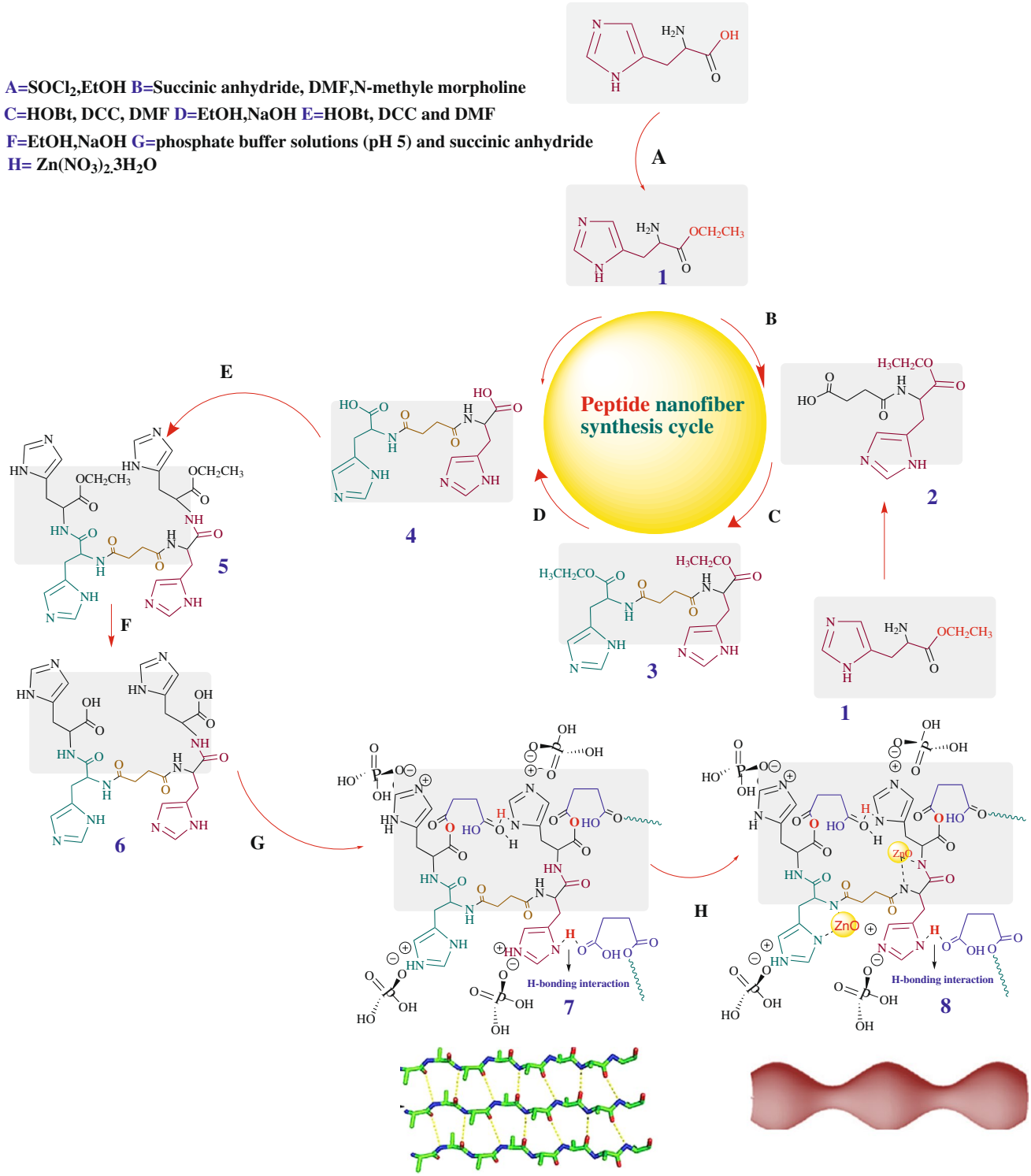

Scheme 1 Schematic synthesis of ZnO nanoparticles supported on the peptide nanofiber

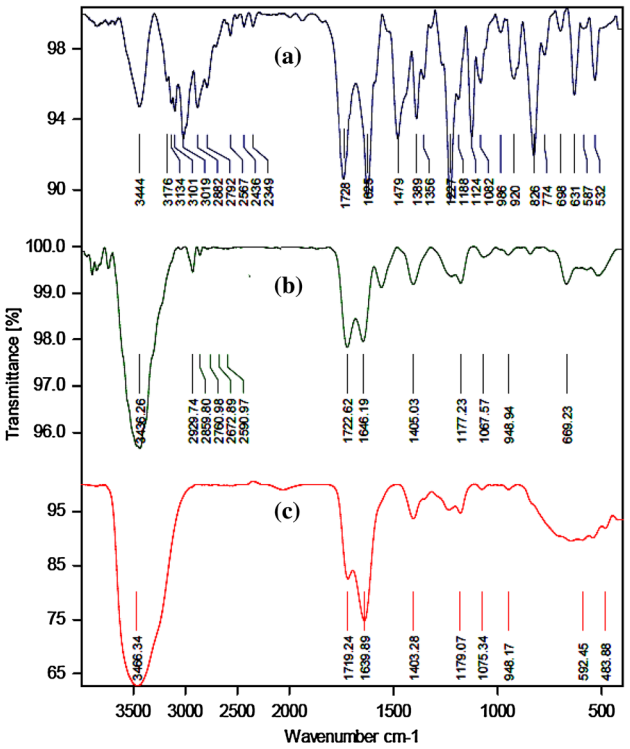

Fig. 1 FT-IR spectra of peptide powder (**a**), the peptide nanofiber (**b**), and peptide nanofibers decorated with ZnO nanoparticles (**c**)

a hexagonal quartzite structure. The peaks have occurred for ZnO at an angle of $2\Theta = 33.3°$ and 34° which leads the crystalline nature [34, 35]. Also, the other peaks related to peptide nanofiber structure which has a different pattern with XRD peak positions related to the peptide nanofiber before adding $Zn(NO_3)_2{\cdot}6H_2O$ this is probably due to the effects of ZnO nanoparticle on morphology of peptide nanofiber.

The optical properties of the peptide nanofiber decorated with Zn were investigated by UV–Vis spectroscopy (Fig. 3). For comparison, UV–Vis spectra of the prepared ZnOPNF, and zinc metallic and peptide nanofiber at room temperature using water as the solvent are also presented in Fig. 2. For peptide nanofiber the observed absorption band at $\lambda = 280–300$ nm is assigned to $\pi–\pi^*$ upon coordination with zinc ions, and there are minor changes of these bands. The visible spectra of the desired peptide nanofiber decorated with zinc show the maximum absorption at 285 nm, which can be assigned to d to d electron transition or metal to ligand charge transfer (MLCT). The presence of Zn metal on the surface of peptide nanofiber was determined, by an EDS technique (Fig. 4). As shown in Fig. 4, the EDS spectrum of ZnO PNF shows the presence of O, C, N and as well as Zn species in the ZnONP-PNF. The morphology of peptide nanofiber decorated with ZnO nanocatalyst was also studied by SEM and TEM techniques (Figs. 5, 6). SEM images of ZnONP-PNF indicate a very uniform size distribution of zinc nanoparticles without agglomeration (Fig. 5). This observation from the TEM image indicates that peptide nanofiber spontaneously changes into metastable necklace-like structures. In order to determine the exact amount of Zn in ZnONP-PNF. ICP-OES was used. From this analysis, the amount of Zn in the catalyst is found to be 2607 ppm or 0.01 g.

3.1 Catalytic Study

To investigate the catalytic activity of the prepared peptide nanofiber decorated with ZnO as a nanocatalyst in

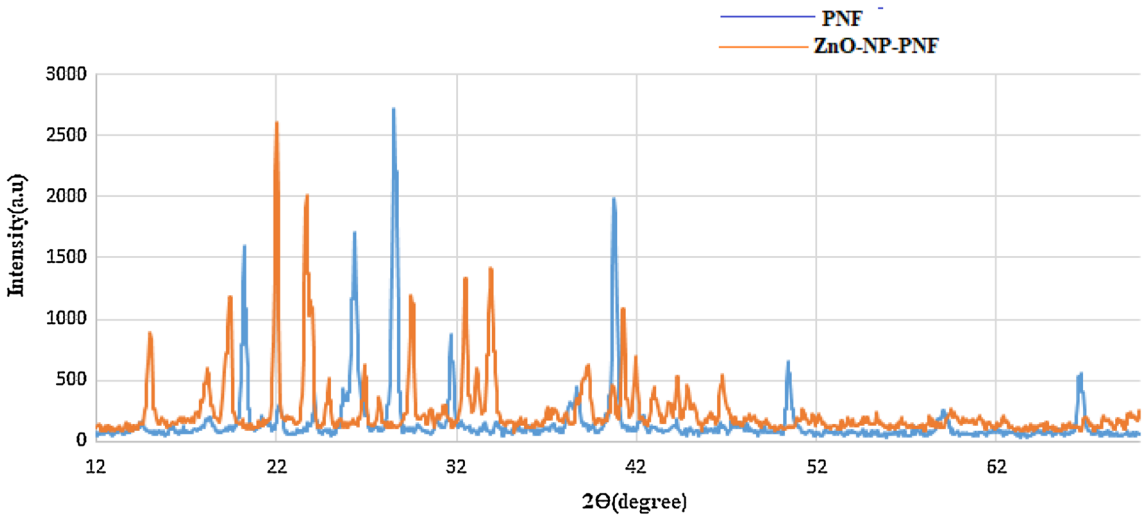

Fig. 2 The X-ray diffraction pattern of peptide nanofiber and ZnO immobilized on peptide nanofibers

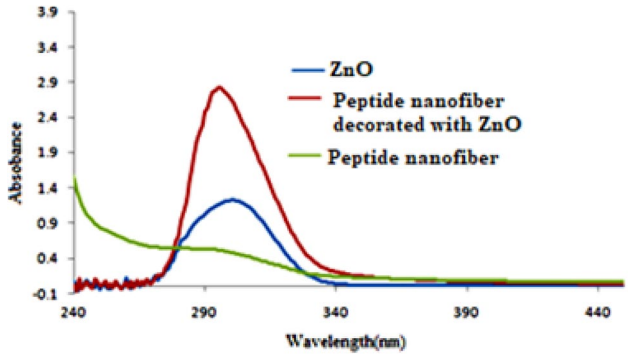

Fig. 3 UV–Visible absorption spectra for $Zn(NO_3)_2{\cdot}6H_2O$, peptide nanofibe and ZnO NP-PNF

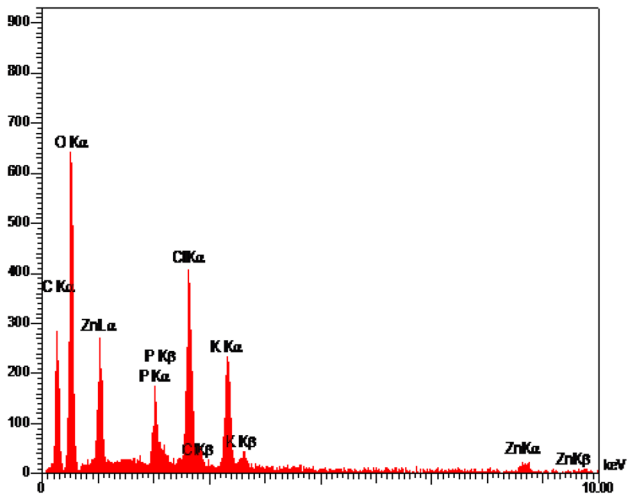

Fig. 4 EDS spectrum of peptide nanofibers decorated with Zn nanoparticles

N-arylation, we started this synthesis by conducting the reaction of aniline and hydroxybenzotriazole, at 130 °C using DMSO in the absence of the catalyst. The progress of the reaction was monitored by TLC. The control experiment confirmed that the reaction did not occur in the absence of the catalyst. When the reaction was conducted in the presence of ZnOPNF, at 130 °C, the desired product was formed. Next, the influence of the amount of catalyst on the yield of the product was evaluated. It was observed that 0.75 mg of peptide nanofiber decorated with ZnO was found to be optimal, a lower yield was observed and a longer reaction time was required when the amount of the catalyst was decreased (entry 11). Increasing the amount catalyst could increase the yield of the desired product (entry 13 and 14). Then, we performed the model reaction using different solvents such as PEG, DMSO, H_2O, DMF, THF, and dioxane, DMSO was found to be the most effective. Among various bases screened, KOH was found to be an excellent base (Table 1, entry 2). Base NaOH was tested and led to the formation of lesser amounts of the desired product. Potassium hydroxide (KOH) in dimethyl sulfoxide (DMSO) forms a superbasic medium that allows to access cross-coupling products from reactions of aryl halides with nitrogen-based nucleophiles by the SNAr mechanism or aryne formation. Among the known superbases, two-phase systems such as an alkali metal hydroxide–dipolar nonhydroxylic solvent are believed to be the most universal, available, stable, and convenient to handle. And among these the KOH/DMSO suspension is the champion. In the light of the presented literature data, we hypothesized that this in situ formed superbase would be active enough to allow arylations of nucleophiles leading to cross-coupling products [35, 36].

We also investigated the effect of temperature on the reaction. When the reaction was conducted at a low temperature, the yields observed were very low (Table 1, entries 10 and 11). The ideal temperature for the reaction was found to be130 °C. The best result was obtained when the reaction was pursued at 130 °C, using 0.75 mg of peptide nanofiber decorated with ZnO in the presence of KOH (5 mmol) and DMSO (2.0 mL). To clarify the especial catalytic activity of ZnONP-PNF in *N*-arylation, in a set of experiments the model reaction was carried out in the presence of $Zn(NO_3)_2{\cdot}3H_2O$ and CuNP-PNF respectively (Table 1). When the reaction was conducted in the presence of $Zn(NO_3)_2{\cdot}3H_2O$ and CuNP-PNF the yield observed was low compared to ZnONP-PNF.

To examine the general applicability of the ZnONP-PNF catalyst for *N*-arylation and the scope of the process, various substituted aliphatic and aromatic amines were investigated, as shown in Table 2.

The second portion of this work involves the application of our protocol to the synthesis of imidazoheterocycles by a three-component reaction of 2-aminopyridine, aldehyde, and terminal alkyne. The reaction of 2-aminopyridine, 4-nitrobenzaldehyde with phenylacetylene was chosen as model substrates to optimize the reaction conditions, and several parameters such as the amount of catalyst, base, solvent, and temperature were screened (Table 3). Firstly, the effect of solvents was investigated and it was observed that the desired product was obtained in the PEG (Table 3, entry 2). The desired product was not obtained in the presence of bases such as KOH, K_2CO_3, Na_2CO_3, Et_3N, and $NaHSO_4$, and even at 130 °C, the yield did not change.

Finally, the amount of *catalyst* was screened, and 0.75 mg of ZnOPNF was found to be optimal (Table 3, entry 2). Encouraged by the above interesting results, we studied the coupling reaction of various aldehydes, 2-aminopyridine and phenylacetylene, under optimized conditions. The results are shown in Table 2. All of the reactions proceeded smoothly to afford the corresponding imidazoheterocycles in good yields. Aromatic aldehydes carrying electron-withdrawing

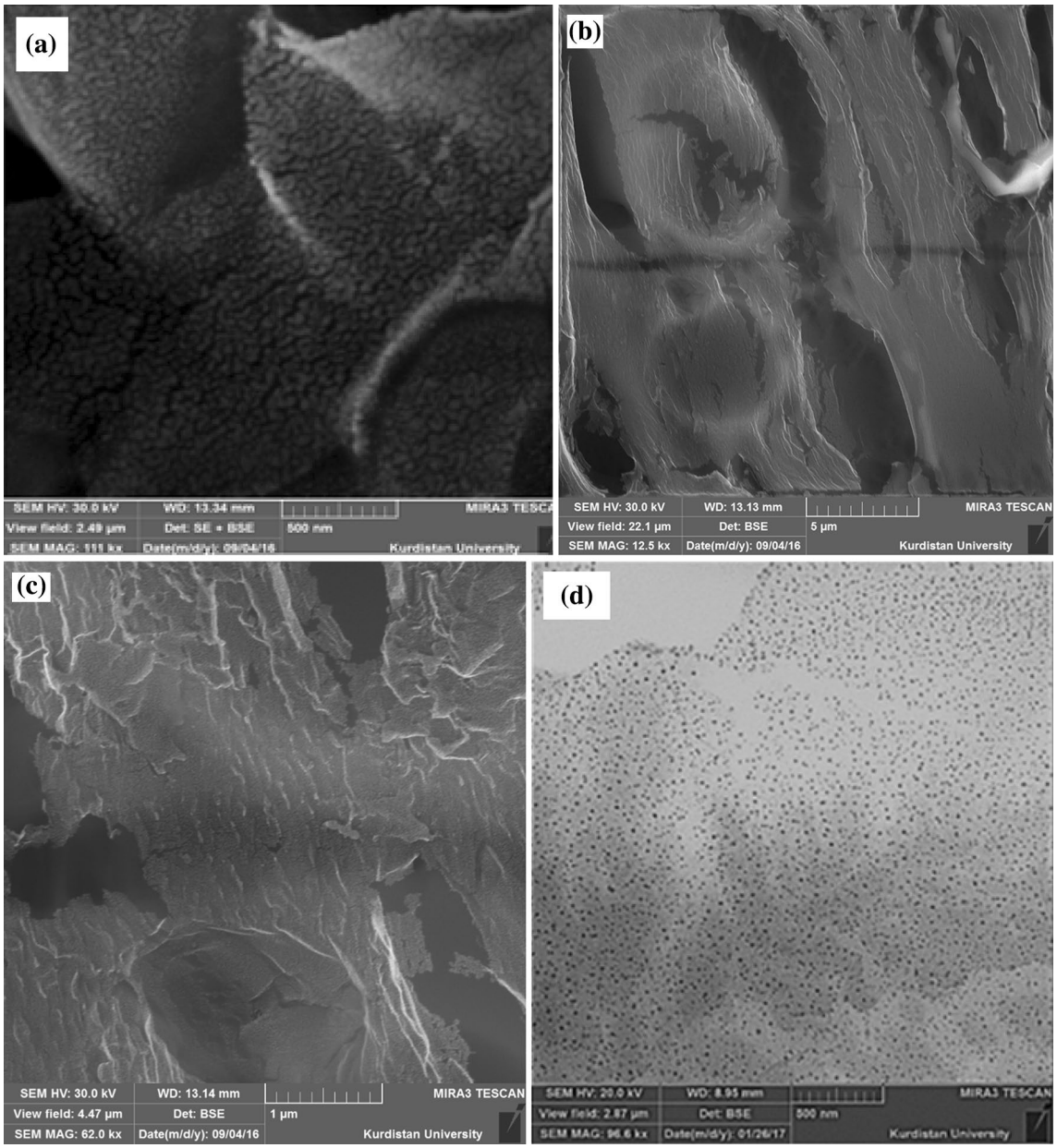

Fig. 5 **a**–**c**SEM images of solution peptide by adding succinic anhydride at pH 5 and **d** SEM image of immobilized ZnO nanoparticles on the surface of the peptide nanofiber

substituents showed reactivity and reacted efficiently to yield the desired product. Moreover, heterocyclic aldehydes such as thiophene-2-carbaldehyde (Table 4, entry 5) also displayed a high reactivity under this standard condition.

A possible mechanism has been proposed for the formations of imidazoheterocycles in Scheme 2. Firstly, imine has been synthesized by condensation of an aldehyde with 2-aminopyridine in the presence of ZnONP-PNF. Then, the resulting products are treated with phenylacetylene to generate propargylamine. Tautomerizes of propargylamine to intermediate **3** is followed by 5-*exo-dig* cyclization to afford **4**, which finally isomerized to product **5**.

Later, the one-pot synthesis of tetracyclic quinazolinone by a three-component reaction of isatoic anhydride, ninhydrin and aromatic and aliphatic amines such as benzylamine, methoxybenzylamine, cyclopropyle, cyclohexyl, cycloctyle, isopropyl, ethylaniline, and aniline were studied. We started quinazolinone synthesis by reaction of benzyl amine, isatoic anhydride, and ninhydrin, as the model case for condition optimization. The results are summarized in Table 5. Initially, various solvents were

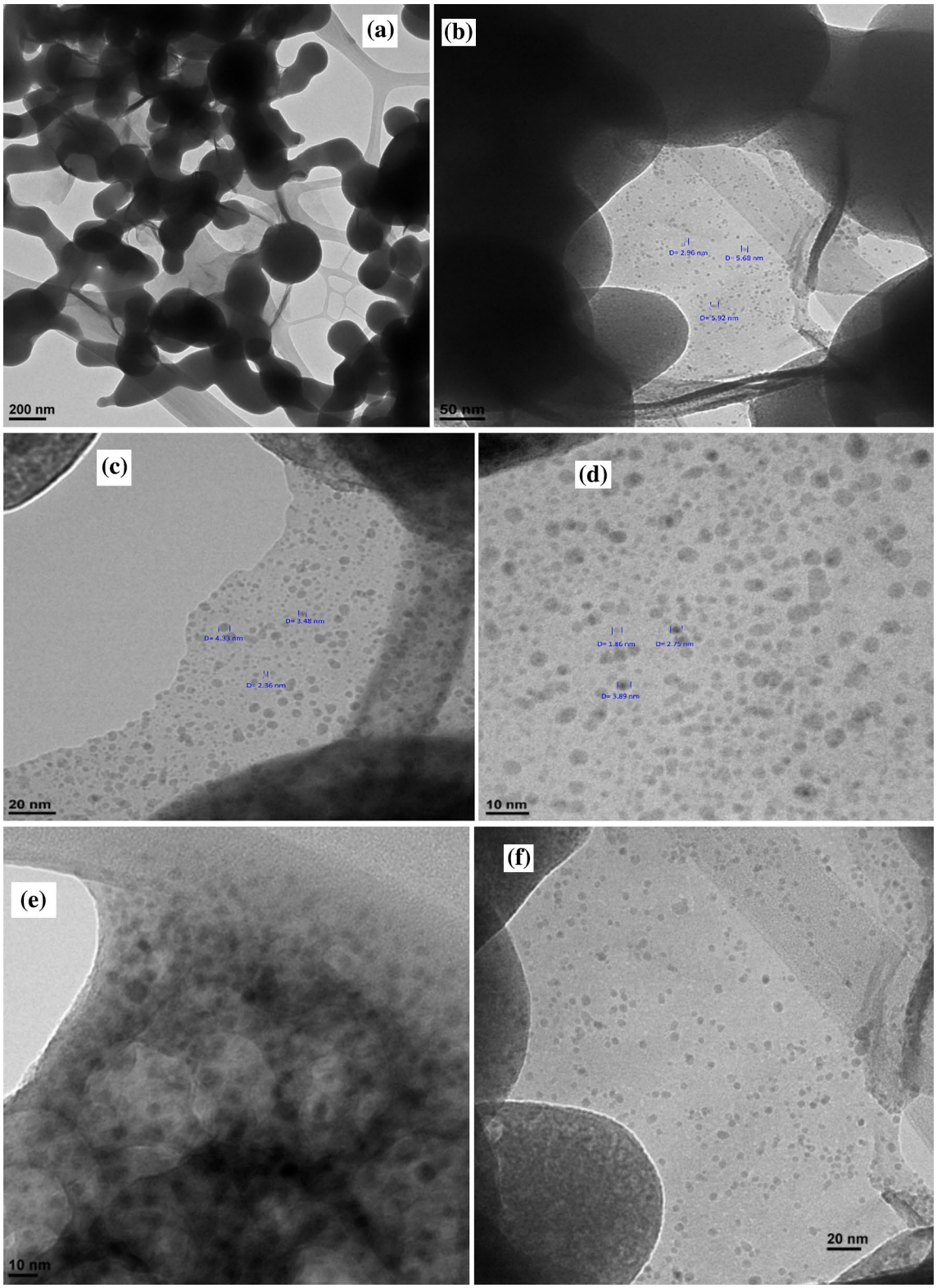

Fig. 6 TEM images of immobilized ZnO nanoparticles on the surface of the woven nanofibers (a–f)

Table 1 Optimization of the reaction conditions for the C–N coupling reaction in the presence of ZnO nanoparticle supported on the peptide nanofiber[a]

Entry[a]	Cat. (mg)	Solvent	Base	Temp. (ºC)	Yield[b] (%)	Time (h)
1	–	DMSO	KOH	130	N.R	10
2	0.5	DMSO	KOH	130	70	10
3	0.5	H_2O	KOH	130	N.R	10
4	0.5	DMF	KOH	130	23	10
5	0.5	THF	KOH	130	N.R	10
6	0.5	PEG	KOH	130	N.R	10
7	0.5	Dioxane	KOH	130	N.R	10
8	0.75	DMSO	KOH	130	80	10
9	0.25	DMSO	KOH	130	50	10
10	0.75	DMSO	KOH	100	68	10
11	0.75	DMSO	KOH	80	15	10
12	0.75	DMSO	NaOH	130	63	10
13	0.75	DMSO	K_2CO_3	130	N.R	10
14	0.75	DMSO	Na_2CO_3	130	N.R	10
15	0.75	DMSO	Et_3N	130	N.R	10
16	0.75	DMSO	KF	130	N.R	10
17[c]	0.75	DMSO	KOH	130	33	10
18[d]	0.75	DMSO	KOH	130	65	10

[a]Reaction conditions: hydroxybenzotriazole (1 mmol), aniline (2 mmol), base 5 mmol

[b]Isolated yield

[c,d]When the reaction was conducted in the presence of $Zn(NO_3)_2{\cdot}3H_2O$ and CuNP-PNF respectively

Table 3 Optimization of the reaction conditions for imidazoheterocycles using 2-aminopyridine, 4-nitrobenzaldehyde and phenyl acetylene[a]

Entry	Cat (mg)	Solvent	Temp. (ºC)	Base	Yield (%)[b]
1	0. 75	DMSO	100	–	N.R
2	0.75	PEG	100	–	80
3	0.75	DMF	100	–	N.R
4	0.75	H_2O	100	–	N.R
5	0.75	PEG	100	Na_2CO_3	N.R
6	0.75	PEG	100	K_2CO_3	N.R
7	0.75	PEG	100	KOH	Trace
8	0.75	PEG	100	Et_3N	N.R
9	0.75	PEG	100	$NaHSO_4$	N.R
10	0.75	PEG	80	–	55
11	0.5	PEG	100	–	58
12	0.25	PEG	100	–	23
13	–	PEG	100	–	N.R

[a]Reaction conditions: 4-nitrobenzaldehyde (1 mmol), 2-aminopyridine (1 mmol), phenyl acetylene (1 mmol), base (2 mmol)

[b]Isolated yield

screened. It was observed that this reaction proceeds well in PEG. In DMF and DMSO, (Table 6, entries 5–7), the yield of the product was less than 50%. The reaction did not occur when conducted at room temperature and 50 °C (Table 5, entries 5 and 6). The ideal temperature for the reaction was found to be 100 °C. Next, the influence of the different amount of catalyst on the reaction was tested, and 0.62 mg of catalyst was found to be optimal. A lower yield was observed when the amount of the catalyst was decreased (Table 5, entry 8). Also, the control experiment confirmed that the reaction did not occur in the absence of the catalyst. With the optimal reaction conditions in hand, we then investigated the scope reaction for synthesis of quinazolinone derivatives and the results are summarized in Table 6. The protocol is applicable to a wide variety

Table 2 Synthesis of secondary amines *via* reaction of hydroxybenzotriazole and amines catalyzed by peptide nanofibers decorated with ZnO nanoparticles (ZnNP-PNF) in DMSO

Entry	Amine	Product	Time (h)	Yield (%)[b]
1	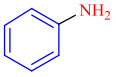	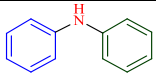	10	80
2	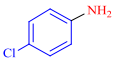	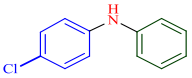	8	88
3	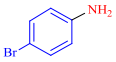	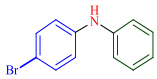	15	53
4	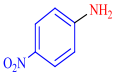	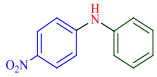	10	63
5		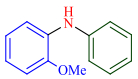	12	55
6	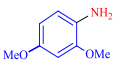	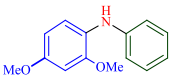	15	47
7	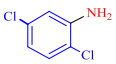	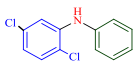	12	68
8	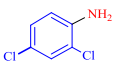	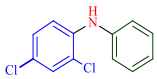	12	53
9	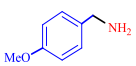	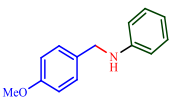	8	73
10		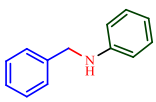	8	78

[a]Reaction conditions: hydroxybenzotriazole (1 mmol), amine (2 mmol), ZnONP-PNF (0.75 mg), KOH 5 mmol, 130 °C

[b]Isolated yield

of aromatic and aliphatic amines providing moderate to excellent yield of desired products.

The possible mechanism for the formation of tetracyclic quinazolinone was proposed as shown in Scheme 3. Attack of the N nucleophile at the electrophilic C of the C=O group of isatoic anhydride related to ring opening and decarboxylation to form compound **B**. Then followed by nucleophilic attack of amine to the keto group of ninhydrin to afford **C**, nucleophilic attack of amine on the keto group provide fused aziridine compound **D**, and the subsequent rearrangement leads to tetraheterocyclic product **F**.

One major advantage of the catalyst is its recyclability and it makes them useful for commercial applications. Therefore, the recovery and reusability of our supported catalyst was investigated in *N*-arylation of aniline with hydroxybenzotriazole under optimized conditions for four runs. The reaction was performed in DMSO at 130 °C, using 1 mmol aniline, 1 mmol hydroxybenzotriazole and 5 mmol KOH in

Table 4 Synthesis of imidazoheterocycles

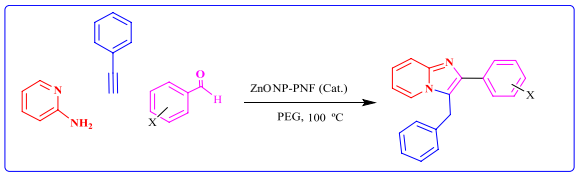

Entry[a]	Amine	Aldehyde	Product	Time (h)	Yield (%)[b]
1		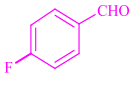	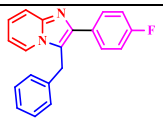	14	55
2	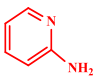	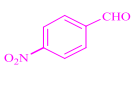	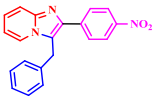	10	85
3		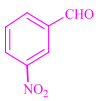	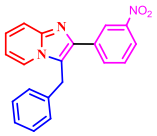	10	88
4		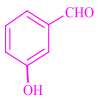	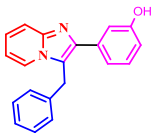	12	95
5		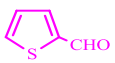	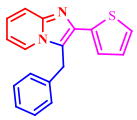	20	63
6			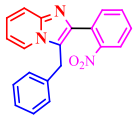	10	75
7		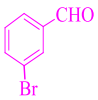	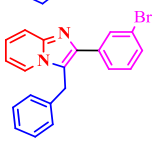	13	90

[a]Reaction conditions: benzaldehyde (1 mmol), 2-aminopyridine (1 mmol), phenyl acetylene (1 mmol) and ZnONP-PNF (0.75 mg)

[b]Isolated yield

the presence of ZnO NP-PNF (0.75 mg), upon completion of the reaction, the mixture was cooled to room temperature. 20 mL of ethyl acetate was added to the reaction mixture, which led to the precipitation of ZnONP-PNF. The resulting precipitate was washed twice with ethyl acetate (2 × 10 mL), dried and applied for the next run. It was found that ZnONP-PNF could be reused at least four times without a significant loss of its catalytic activity (Fig. 7).

Also the morphology of peptide nanofiber templated ZnO nanostructures the recovered for for130 °C reaction temperature was studied by SEM technique (Fig. 8). It was easily observed that solvent evaporation leads to larger fiber diameters. It is worth mentioning that previous analytical, empirical, and numerical studies suggest that fiber diameter is reduced by decreasing viscosity [37–39].

4 Conclusions

In summary, we describe a simple and ‘‘green’’ method for the synthesis of peptide nanofiber decorated with ZnO. FT-IR, EDS, SEM, TEM, ICP-OES (inductively coupled plasma optical emission spectrometry), and ultraviolet–visible (UV–Vis) spectroscopy results proved that peptide nanofiber decorated with ZnO was formed. TEM

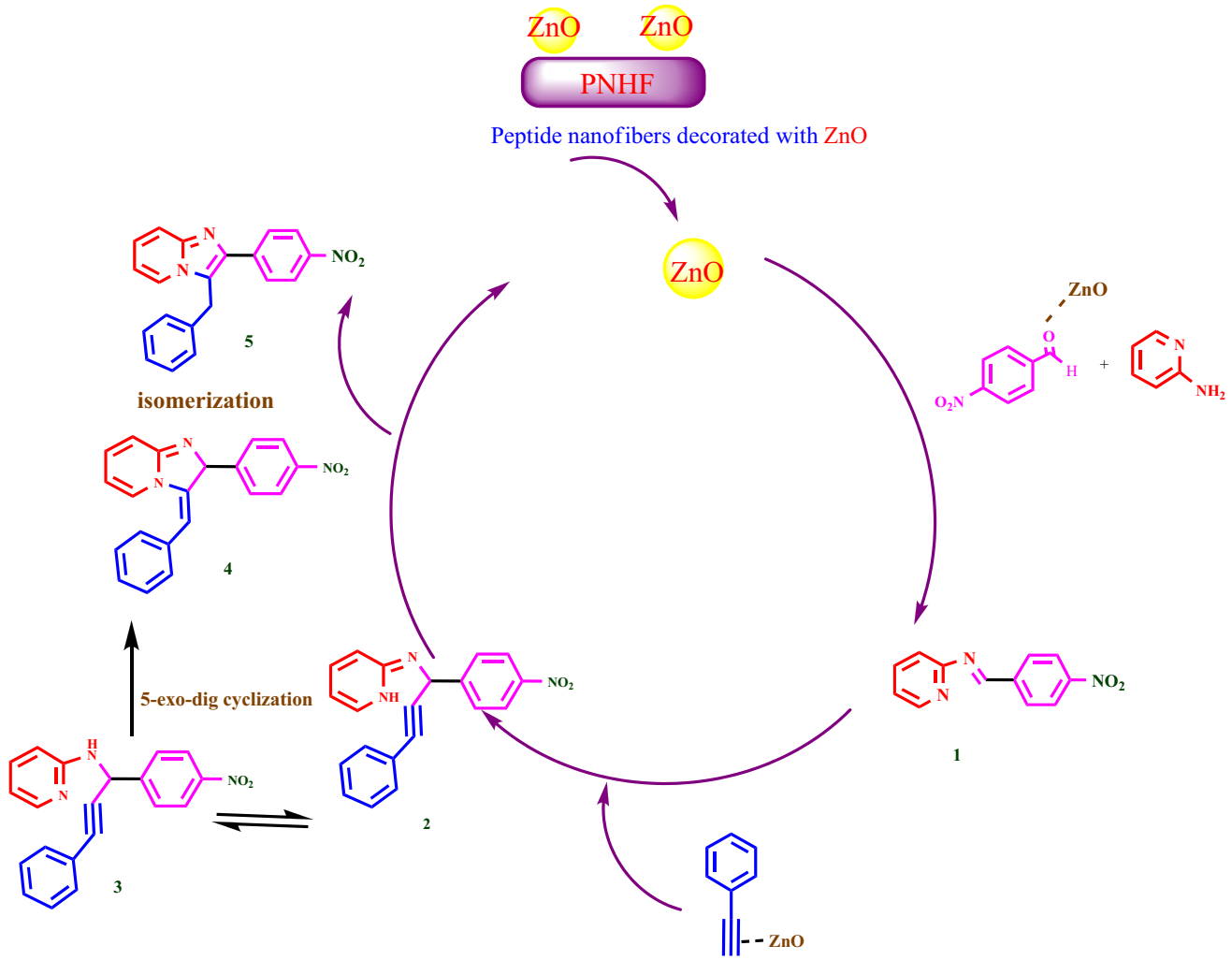

Scheme 2 Proposed mechanism for the synthesis of imidazo [1,2-a] pyridine through three-component reaction of 2-aminopyridine, aldehyde and phenyl acetylene catalyzed by ZnOPNF

Table 5 Optimization of the reaction conditions for tetracyclic quinazolinone using isatoic anhydride, ninhydrin and benzyl amine[a]

Entry	Cat (mg)	Solvent	Temp. (°C)	Yield (%)[b]
1	0.62	DMSO	100	44
2	0.62	PEG	100	78
3	0.62	DMF	100	23
4	0.62	Dioxane	100	N.R
5	0.62	H_2O	100	N.R
5	0.62	PEG	25	N.R
6	0.62	PEG	50	N.R
7	0.62	PEG	80	63
8	0.25	PEG	100	44
9	–	PEG	100	N.R

[a]Reaction conditions: isatoic anhydride (1 mmol), ninhydrin (1 mmol), solvent (2 mL)

[b]Isolated yield (Time 8 h)

images showed the necklace model for peptide nanofiber decorated with ZnO. Peptide nanofibers provide a favorable environment for the synthesis of metal nanoparticles without adding any further stabilizer. Peptide nanofiber decorated with ZnO can catalyze *N*-arylation of aryl halides using hydroxybenzotriazole as a *phenylating reagent*, synthesis of imidazoheterocycles and tetracyclic quinazolinon. High yields, low cost of catalyst, environmental friendliness, efficient recovery and recyclability of catalyst are the most important features of this catalytic system.

Table 6 Synthesis of tetracyclic quinazolinone

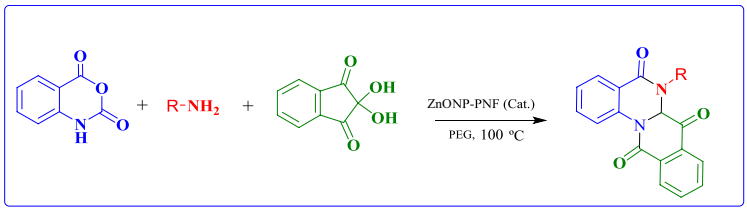

Entry[a]	Amine	product	Time (h)	Yield[b]
1	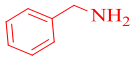	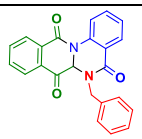	8	78
2	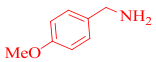	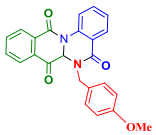	8	90
3		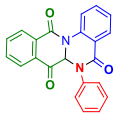	9	85
4	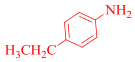	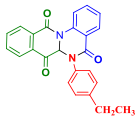	10	75
5	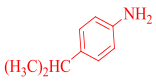	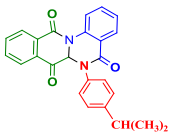	10	90
6	$CH_3CH_2CH_2CH_2NH_2$	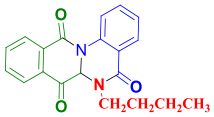	7	55
7		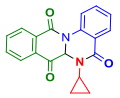	12	80
8	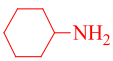	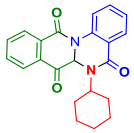	14	78
9	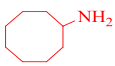	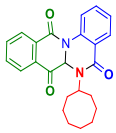	15	69

[a]Reaction conditions: isatoic anhydride (1 mmol), ninhydrin (1 mmol), ZnONP-PNF (0.625 mg), PEG (2 mL)

[b]Isolated yield

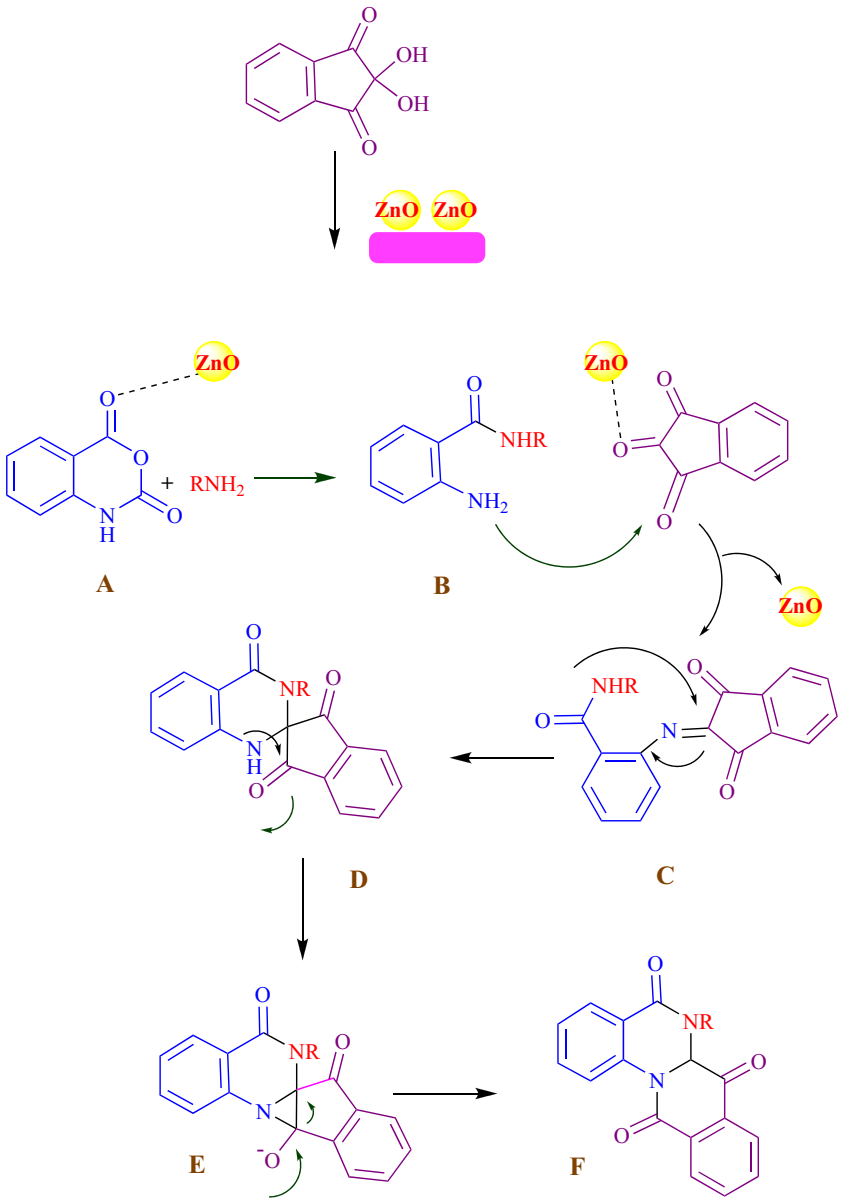

Scheme 3 Proposed mechanism for the synthesis of tetracyclic quinazolinone through three-component reaction of benzyl amine with isatoic anhydride and ninhydrin catalyzed by peptide nanofiber decorated with ZnO nanoparticles

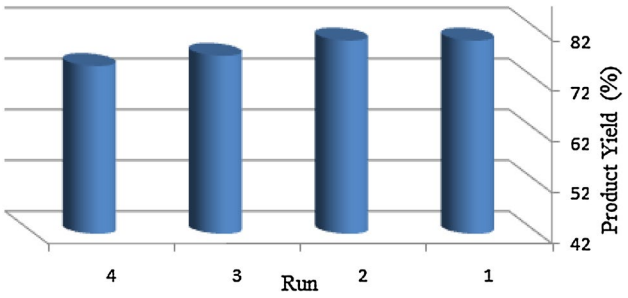

Fig. 7 Catalyst recycling study for *N*-arylation of aniline

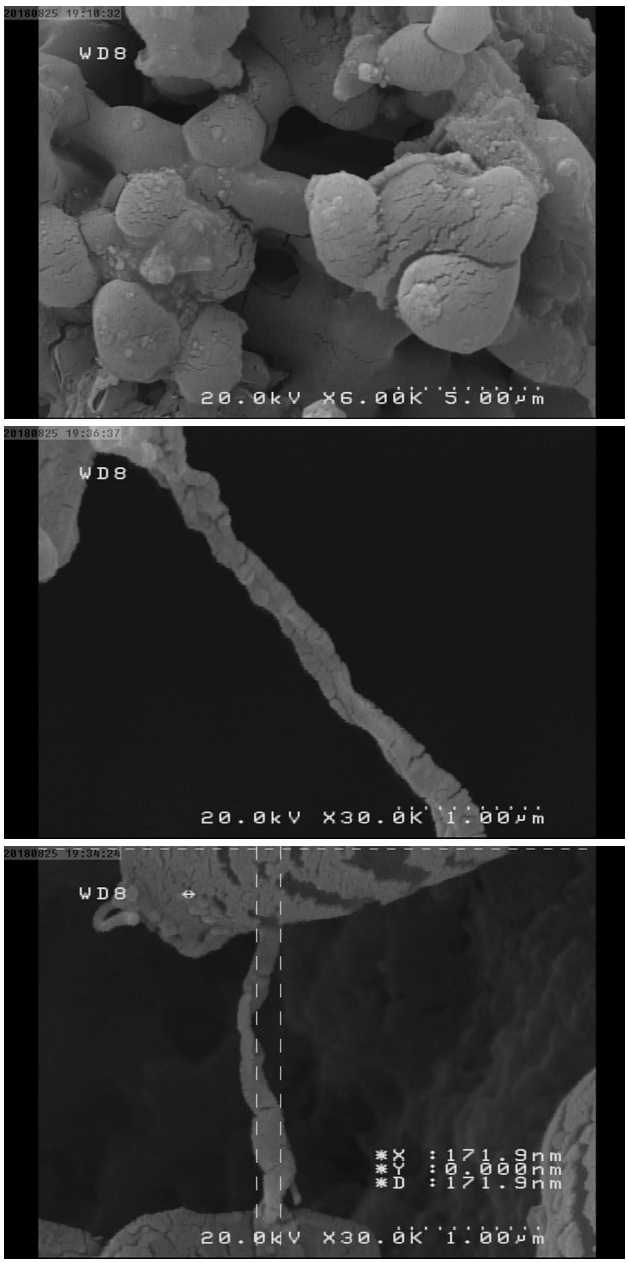

Fig. 8 SEM image of peptide nanofiber decorated with ZnO after recycling

Funding This work was supported by Ilam University

References

1. Hili R, Yudin AK (2006) Nat Chem Biol 2:284
2. Ruiz-Castillo P, Buchwald SL (2016) Chem Rev 116:12564
3. Kumar A, Bishnoi AK (2015) RSC Adv 5:20516
4. Aubin Y, Fischmeister C, Thomas CM, Renaud JL (2010) Chem Soc Rev 39:4130
5. Polprasert C, Liyanage LRJ (1996) Resour Conserv Recycl 16:213
6. Deep A, Kaur Bhatia R, Kaur R, Kumar S, Kumar Jain U, Singh H, Kishore Deb P (2017) Curr Top Med Chem 17:238
7. Starrett JE Jr, Montzka TA, Crosswell AR, Cavanagh RL (1998) J Med Chem 32:2204
8. Chandra Mohan D, Nageswara Rao S, Adimurthy S (2013) J Org Chem 78:1266
9. Reddy BS, Reddy PS, Reddy YJ, Yadav JS (2011) Tetrahedron Lett 52:5789
10. Guo P, Huang S, Mo J, Chen X, Jiang H, Chen W, Zhan H (2017) Catal Commun 90:43
11. Guchhait SK, Chandgude AL, Priyadarshani G (2012) J Org Chem 77:4438
12. Chernyak N, Gevorgyan V (2010) Angew Chem Int Ed 49:2743–2746
13. Asif M (2014) Int J Med Chem. https://doi.org/10.1155/2014/395637
14. Hisano T, Ichikawa M, Kito G, Nishi T (1972) Chem Pharm Bull 20:2575
15. Murthy NV, Nikumbh SP, Kumar SP, Chiranjeevi Y, Rao LV, Raghunadh AA (2016) Synlett 27:2362
16. Shen C, Man NY, Stewart S, Wu XF(2015) Org Biomol Chem 13:4422
17. Yao J, Yao Y (2017) Int J Hydrog Energy 42:18560
18. Ghorbani-Choghamarani A, Morad Pi, Tahmasbi B (2016) RSC Adv 6:56638
19. Scott RW, Ye H, Henriquez RR, Crooks RM (2003) Chem Mater 15:3873
20. Salavati H, Rasouli N (2011) Mater Res Bull 46:1853
21. Gong T, Qin L, Zhang W, Wan H, Lu J, Feng H (2015) J Phys Chem C 119:11544
22. Ghorbani-Choghamarani A, Taherinia Z (2017) Chin J Catal 38:469
23. Eskandari S, Guerin T, Toth I, Stephenson RJ (2017) Adv Drug Deliv Rev 110:169
24. Ren K, Wang Y, Sun T, Yue W, Zhang H (2017) Mater Sci Eng C 78:324
25. Vasita R, Katti DS (2006) Int J Nanomed 1:15
26. Wang W, Anderson CF, Wang Z, Wu W, Cui H, Liu CJ (2017) Chem Sci 8:3310
27. Maity I, Manna MK, Rasale D, Das AK (2014) ChemPlusChem 79:413
28. Wang C, Sun Y, Wang J, Xu H, Lu JR (2015) Chem Asian J 10:1953
29. Acar H, Garifullin R, Aygun LE, Okyay AK, Guler MO (2013) J Mater Chem A 1:10979
30. Khalily MA, Ustahuseyin O, Garifullin R, Genc R, Guler R (2012) Chem Commun 48:11358
31. Kim S, Cho HJ, Lee N, Lee YS, Shin DS, Lee SM (2017) RSC Adv 7:33162
32. Suresh J, Pradheesh G, Alexramani V, Sundrarajan M, Hong SI (2018) Adv Nat Sci 9:015008
33. Dhole SG, Dake SA, Prajapati TA, Helambe SN (2018) Proc Manuf 20:127

34. Chithra MJ, Sathya M, Pushpanathan K (2015) Acta Metall Sin (Engl Lett) 28:394
35. Yuan Y, Thome I, Kim SH, Chen D, Beyer A, Bonnamour J, Bolm C (2010) Adv Synth Catal 352:2892
36. Trofimov BA (1992) J Sulfur Chem 11:207
37. Mellado P, McIlwee HA, Badrossamay MR, Goss JA, Mahadevan L, Kit Parker K (2011) Appl Phys Lett 99:203107
38. Padron S, Fuentes A, Caruntu D, Lozano K (2013) J Appl Phys 113:024318
39. Golecki HM, Yuan H, Glavin C, Potter B, Badrossamay MR, Goss JA, Parker KK (2014) Langmuir 30:13369